Journal of NeuroVirology (2000) 6, Suppl 1, S44–S52

www.jneurovirol.com

Biphasic and regionally-restricted chemokine expression in the central nervous system in the Theiler's virus model of multiple sclerosis

Paul D Murray*[,1], Kim Krivacic[3], Ann Chernosky[3], Tao Wei[3], Richard M Ransohoff[3,4] and Moses Rodriguez[1,2]

[1]Department of Immunology, Mayo Clinic and Foundation, Rochester, Minnesota, MN 55905, USA; [2]Department of Neurology, Mayo Clinic and Foundation, Rochester, Minnesota, MN 55905, USA; [3]Department of Neurosciences, The Lerner Research Institute, Cleveland Clinic and Foundation, Cleveland, Ohio, USA and [4]Department of Neurology (Mellen Center for MS Treatment and Research), Cleveland Clinic and Foundation, Cleveland, Ohio, USA

Intracerebral infection of susceptible strains of mice with Theiler's murine encephalomyelitis virus (TMEV) induces a biphasic disease characterized by acute polioencephalitis followed by chronic demyelination and viral persistence in the spinal cord white matter. There has been limited study of soluble mediators responsible for the initial recruitment of inflammatory cells into the gray matter, and the secondary influx into the white matter during infection with TMEV. We used sensitive and specific RT–PCR/dot blot hybridization assays to quantitate the relative levels of chemokine mRNA in the brains and spinal cords during the acute and chronic phases of TMEV infection in mice susceptible (B10.M, H-2^f) and resistant (B10, H-2^b) to virus-induced demyelination. TMEV infection resulted in robust expression of mRNA for IP-10, RANTES, and MCP-1, but not GRO-α, in brains and spinal cords in both strains of mice within 5 days. By day 21, virus was cleared, inflammation reduced, and expression of all three chemokines subsided to baseline levels in the brains and spinal cords of resistant mice, and the brains of susceptible mice. Chemokine expression was also reduced in the spinal cords of susceptible mice, corresponding to a shift in TMEV replication from the gray to the white matter. During the chronic, demyelinating phase of infection, there was a resurgence in IP-10, RANTES, and MCP-1 mRNA in spinal cords of susceptible B10.M mice. This study demonstrates the coordinated regulation and regionally restricted expression of chemokines in a biphasic disease of the central nervous system and provides greater understanding of the mechanism by which inflammation is established and maintained in the CNS. *Journal of NeuroVirology* (2000) **6,** S44–S52.

Keywords: demyelination; TMEV; MS; encephalomyelitis; mice; chemoattractants; picornavirus

Introduction

Intracerebral infection with Theiler's murine encephalomyelitis virus (TMEV), induces a biphasic disease consisting of transient neuronal polioencephalitis in all strains that is followed by chronic demyelination in mice with susceptible (H-2^{f,p,q,r,s,v}). In contrast, resistant mice of (H-2^{b,d,k}) MHC haplotypes (Rodriguez *et al*, 1987) develop neuronal infection but the virus is cleared and the demyelination does not develop. Lymphocyte subsets and cytokines involved in TMEV pathogenesis have been extensively characterized (reviewed in Drescher *et al*, 1997; Monteyne *et al*, 1997; Tsunoda and Fujinami, 1996). However, the soluble mediators responsible for initiating inflammation during the acute stage, and maintaining leukocyte extravasation in the CNS during the demyelinating phase of TMEV infection have not been well characterized.

Chemokines (chemoattractant cytokines) are soluble, proinflammatory mediators which selectively induce recruit leukocytes along concentration gradients. Chemokines are secreted by diverse cell types including monocytes/macrophages, lymphocytes, neutrophils, fibroblasts, endothelial cells, keratinocytes, astrocytes, and neoplastic cells (Ransohoff *et al*, 1996) in response to multiple

*Correspondence: M Rodriguez, Department of Immunology and Neurology, Mayo Clinic, 200 First St SW, Rochester, Minnesota, MN 55905, USA

stimuli including LPS, IL-1. TNFα, IFNγ, and PDGF (Tani and Ransohoff, 1994). Chemokine subfamilies are defined by the organization of four positionally-conserved cysteine residues (Tani and Ransohoff, 1994). In the alpha subfamily the cysteines are separated by a single amino acid (C-X-C), and in the beta subfamily (C-C), they are adjacent (Ransohoff *et al*, 1996).

We investigated chemokine expression in acute and chronic TMEV-induced CNS inflammation in susceptible B10.M (H-2^f) and resistant B10 (H-2^b) mice of otherwise identical genetic background. We examined IP-10, an α-chemokine specific for activated T cells (Taub *et al*, 1993), RANTES, a β-chemokine specific for memory T cells and monocytes (Schall *et al*, 1990), MCP-1, a β-chemokine with major specificity for monocytes and T cells (Yoshimura *et al*, 1989; Carr *et al*, 1994; Rollins *et al*, 1991), and GRO-α, an α-chemokine specific for neutrophils (Lira *et al*, 1994). CNS chemokine expression paralleled the distribution and biphasic course of the TMEV-induced demyelinating disease. Expression of mRNA for IP-10, RANTES, and MCP-1, but not GRO-α, were maximally expressed during acute (5 days) disease in both susceptible B10.M and resistant B10 mice. Chemokine expression returned to near baseline levels and coincided with resolution of disease in B10 mice at 21 days. Chemokine expression diminished in spinal cords of B10.M during the shift of virus replication from the gray matter to the white matter (21 days), but was increased at 45 days corresponding to the chronic phase of immune-mediated myelin destruction.

Results

Phasic chemokine expression in the CNS of TMEV-infected mice

Intracerebral infection with TMEV induces transient neuronal polioencephalitis followed by chronic demyelination and viral persistence in the spinal cord white matter of susceptible strains. To determine if chemokine expression paralleled viral pathogenesis in the CNS, we quantitated the relative levels of chemokine mRNA in the brains and spinal cords of susceptible B10.M and resistant B10 mice at 5, 21, and 45 days after infection with TMEV. During the acute stage of infection there was a dramatic increase in expression of IP-10, RANTES and MCP-1, but not GRO-α, mRNA in the brains of both strains (Figure 1). Expression of MCP-1 in the brain was significantly greater in B10 mice *vs* B10.M mice ($P<0.05$ by Student's *t*-test). RANTES expression tended to be higher in B10 brains but this difference was not statistically significant (P=0.063 by Student's *t*-test). At 21 and 45 days p.i., chemokine mRNAs had declined to baseline levels in the brains from both strains. IP-10, RANTES and MCP-1 but not

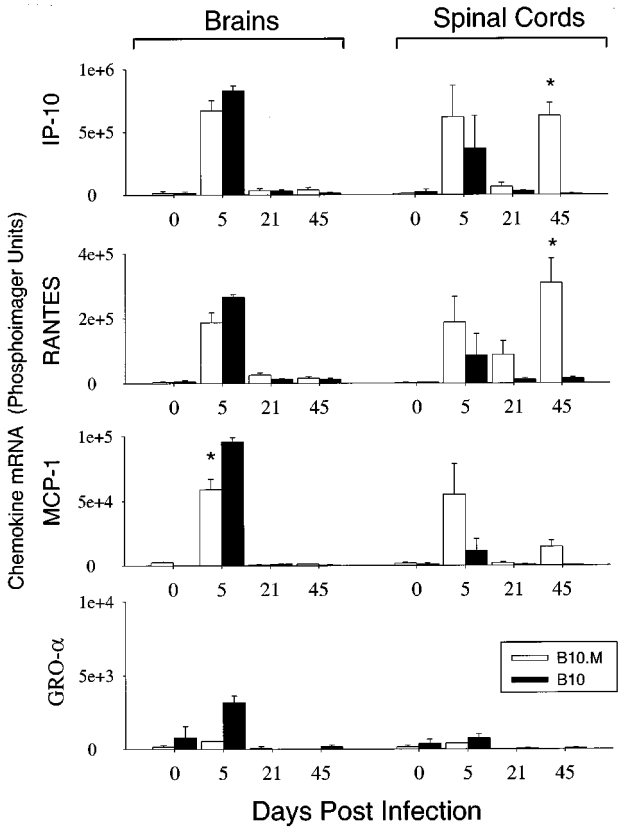

Figure 1 Chemokine expression during the acute and chronic phases of TMEV infection in susceptible and resistant strains. Reverse transcriptase coupled PCR and dot-blot hybridization were used to quantitate relative levels of RNA for the chemokines IP-10, RANTES, MCP-1, and KC/GRO in 30 μm thick cryostat sections from brains and spinal cords of B10.M (open bars) and B10 (solid bars) mice at 5, 21, and 45 days following infection. Expression of IP-10, RANTES, and MCP-1 was elevated in both the brains and the spinal cords relative to controls. By 21 days chemokine expression returned to baseline in both brains and spinal cords of susceptible and resistant strains. By 45 days, IP-10 and RANTES, were highly elevated and MCP-1 was slightly elevated relative to baseline in the spinal cords of susceptible B10.M mice, but not resistant B10 mice. GRO-α was not expressed in an appreciable amount at any time point. Day 0 p.i. indicates uninfected control mice. *Statistical significance ($P<0.05$) between B10.M and B10 mice using the Student's *t*-test.

GRO-α, mRNA were also expressed in the spinal cords by 5 days (Figure 1), although to a lesser extent in B10 *vs* B10.M mice. By 21 days, expression of all three chemokines had returned to baseline in the spinal cords of B10 mice, and were greatly diminished in the spinal cords of B10.M mice. By 45 days, IP-10 and RANTES RNA were elevated to levels observed in the acute phase of disease in spinal cords of B10.M mice and were greater than observed in B10 mice at the same time point ($P<0.05$ by Student's *t*-test). Expression of MCP-1 also increased above the level observed at 21 days, but failed to attain

levels detected during the acute stage. GRO-α was not elevated at any time point.

Inflammation and viral clearance from the brains of susceptible and resistant strains

To determine the relationship between chemokine expression and disease pathogenesis, we examined brains of B10.M and B10 mice. At day 5, inflammation was widespread in both strains, and tissue destruction was most frequently detected in the hippocampus, striatum, and corpus callosum (Figure 2A,B). Necrosis was more frequent in B10 mice (Figure 2A,B), however inflammation characterized by perivascular cuffing, parenchymal infiltration, and tissue destruction was readily detected in both strains (Figure 3A,B). *In situ* hybridization revealed virus RNA was abundant in the striatum of B10.M (Figure 3E) and B10 (Figure 3F) mice. By 21 days, inflammation had decreased in both strains (Figure 2C,D). B10.M mice demonstrated some persistent inflammation but parenchymal damage was infrequent, and in B10 mice, only scattered focal brain lesions remained. At this time point, viral RNA was not detected in brains from either strain (Figure

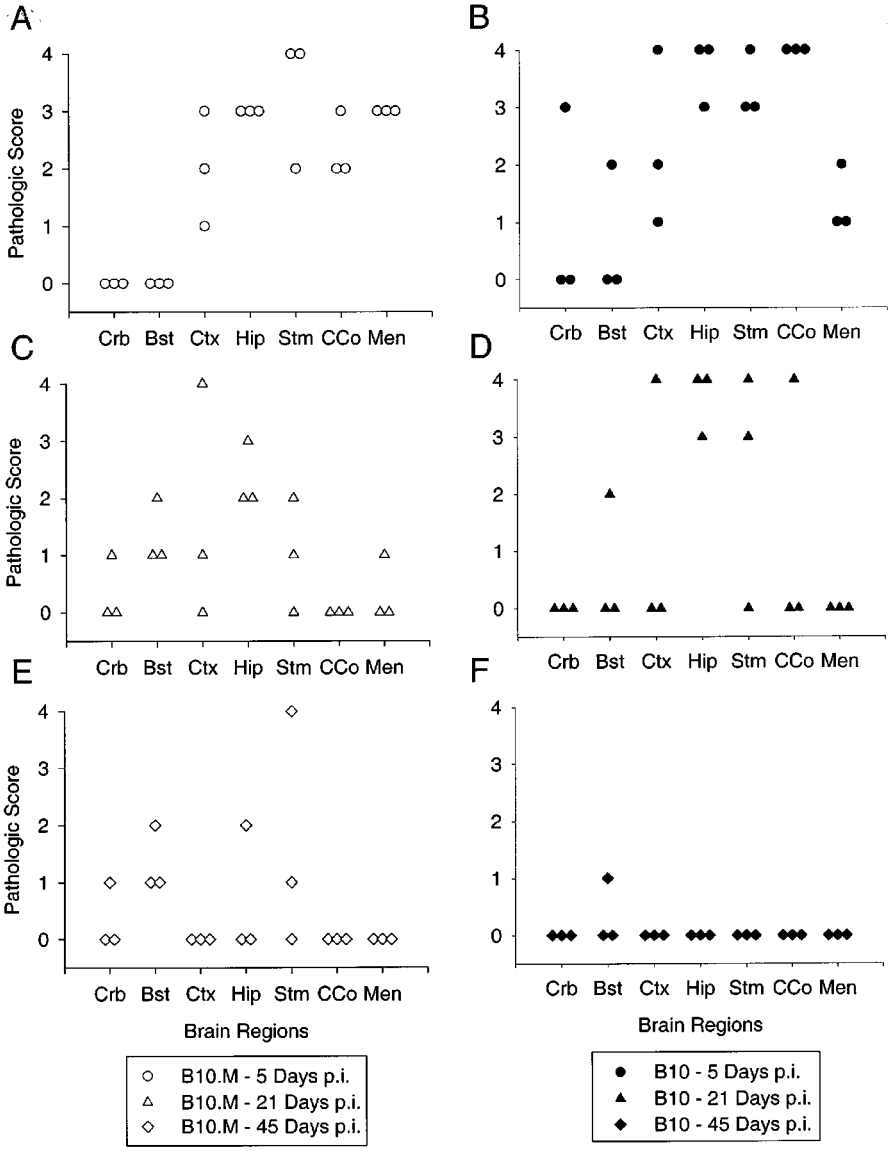

Figure 2 Quantitation of brain pathology in mice susceptible and resistant to chronic demyelinating disease 5, 21, and 45 days after TMEV infection. Brains from susceptible B10.M (open symbols) and resistant B10 mice (closed symbols) infected for 5 (**A,B**), 21 (**C,D**) and 45 (**E,F**) days were analyzed. The cerebellum (Crb), brainstem (Bst), cerebral cortex (Cor), hippocampus (Hip), striatum (Stm), corpus callosum (Cco), and meninges (Men) were graded independently on a four-point scale for the presence of inflammation, demyelination and necrosis as described in Materials and methods. Severe inflammation and tissue destruction were observed in 5-day infected B10.M (**A**) and B10 (**B**) mice. Inflammation with parenchymal disease was reduced in both strains by 21 days (**C,D**), and had resolved by 45 days (**E,F**).

3G,H). By 45 days, most of the inflammation had resolved (Figure 2E,F), minimal evidence of prior insult remained (Figure 3C,D) and virus had been cleared (data not shown). Residual inflammation

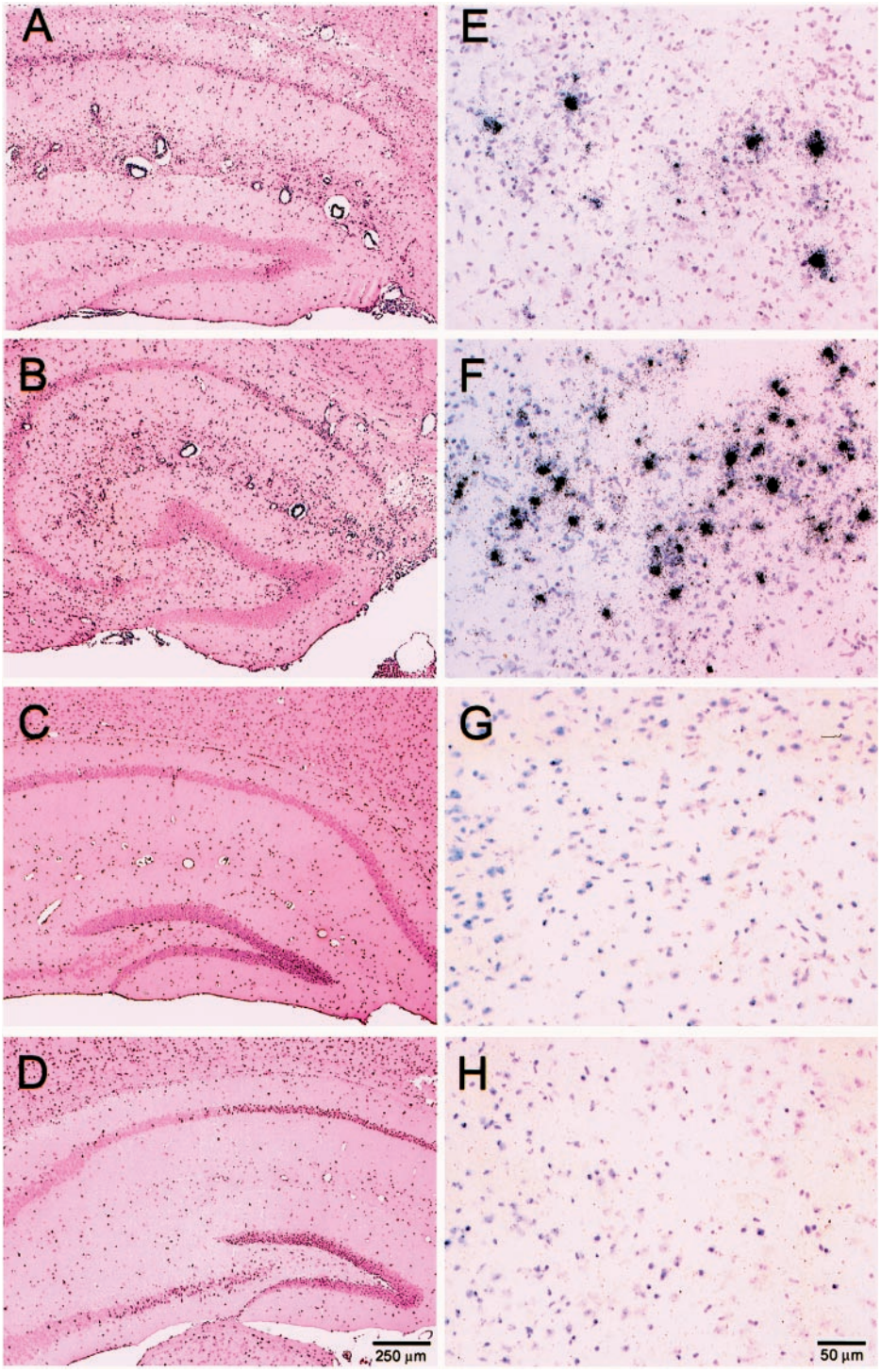

Figure 3 Acute inflammation with parenchymal infiltration and tissue destruction and viral replication resolves in the brains of B10.M and B10 mice following infection with TMEV. Hematoxylin and eosin-stained coronal brain sections from susceptible B10.M (**A,C**) and resistant B10 (**B,D**) mice infected for 5 (**A,B**), and 45 (**C,D**) days were analyzed. Five days following infection perivascular and parenchymal infiltration with tissue destruction was observed in the hippocampi of both B10.M (**A**) and B10 (**B**) mice. By 45 days following infection, inflammation had resolved in brains from both B10.M (**C**) and B10 (**C**) mice, and minimal evidence of residual tissue destruction was observed. *In situ* hybridization with a ^{35}S-labeled probe specific for the VP1 region of TMEV demonstrates TMEV mRNA in the striatum of B10.M (**E**) and B10 (**F**) mice. By 21 days, virus mRNA was undetectable in either the B10.M (**G**) or the B10 (**H**) strain.

was primarily localized in brainstem of susceptible B10.M mice, an observation characteristic of chronic TMEV persistence. Results from *in situ* hybridization were similar to those obtained using immunostaining for viral antigen (data not shown).

Pathology and viral persistence in spinal cords of susceptible and resistant strains

Resistant strains clear virus from the CNS, while susceptible strains develop chronic viral persistence and myelin destruction in the white matter (Njenga *et al*, 1997). Spinal cords from 5-day-infected mice demonstrated inflammation in the gray matter of both strains (Table 1) characterized by infiltration by mononuclear cells and neuronophagia (Figure 4A,B). TMEV RNA (Figure 4E) and antigen were frequently observed in the gray matter of B10.M mice (three of three and two of three, respectively), but were less common in resistant B10 mice (one of three) (Figure 4F). At 21 days, inflammatory cells were detected in both the gray and white matter in B10.M mice however inflammation had largely resolved in the gray matter of B10 mice and was not detected in the white matter. TMEV was detected by *in situ* hybridization (one of three), and immunostaining (two of three) in B10.M mice, but not B10 mice at 21 days (data not shown). By 45 days, focal demyelinating lesions characterized by infiltration with mononuclear phagocytes and lymphocytes were present in nearly 20% of quadrants of spinal cord axial sections from B10.M mice (Table 1, Figure 4C) while inflammation had completely resolved in B10 mice (Table 1, Figure 4D). At this time point virus was readily detected in the spinal cord white matter in each of three B10.M mice by *in situ* hybridization (Figure 4G) and immunohistochemistry (data not shown), but not B10 mice (Figure 4H).

Table 1 Quantitation of spinal cord pathology in B10.M and B10 mice

Strain	*Days*	N	*Gray matter inflammation*	*Meningeal inflammation*	*Demyelination*
B10.M	5	3	5.2±2.3	3.5±1.9	1.2±1.2
B10	5	3	8.3±0.9	3.2±1.3	0.0±0.0
B10.M	21	3	7.6±1.0*	5.5±1.3	7.1±3.8
B10	21	3	0.8±0.8	0.0±0.0	0.5±0.5
B10.M	45	3	1.1±0.6	2.3±1.1	18.6±3.4*
B10	45	5	0.0±0.0	0.0±0.0	0.4±0.4

Demyelination, gray matter inflammation and meningeal inflammation were assessed in spinal cord coronal sections (12–15/mouse). Data are the per cent of quadrants expressing the pathologic abnormality±s.e.m. *N*=number of mice. *Statistically significant difference ($P<0.05$ by Student's *t*-test) of B10.M mice *vs* B10 mice.

Discussion

This paper describes the coordinated regulation and regionally restricted expression of chemokines following TMEV infection of the central nervous system. In brains of B10 and B10.M mice, genes for IP-10, RANTES, and MCP-1 were rapidly expressed but returned to baseline by 21 days p.i. In B10.M brains, chemokine expression subsided despite residual inflammatory cells brains and ongoing virus replication, chemokine expression, and pathology in the spinal cords of B10.M mice. The differential expression of specific chemokines in each phase of TMEV infection was remarkable. Although chemokine expression was somewhat elevated in brains of B10 *vs* B10.M mice at 5 days, this was not observed in spinal cords, possibly due to strong, protective response by cytotoxic lymphocytes that prevent viral replication in the spinal cord of resistant strains. Despite the transient decrease in expression at day 21, IP-10 and RANTES, and to a lesser extent MCP-1, were again expressed at high levels in spinal cords of susceptible strains in the chronic stage of disease. The neutrophil-specific α-chemokine GRO-α (Lira *et al*, 1994) was not expressed at significant levels in the CNS at any time point corresponding to the absence of polymorphonuclear leukocytes in the inflammatory infiltrate. Therefore, chemokine expression corresponded with (1) the temporal profile of disease, (2) the spatial location (brain *vs* spinal cord), (3) the natural history of the disease (susceptible *vs* resistant strains), and (4) the nature of the inflammatory response inflammation (T cells and monocytes *vs* PMNs). These observations demonstrate temporal and spatial regulation of chemokine expression that corresponds with the antiviral host response and demyelinating pathology.

The study of chemokine expression following infection with other CNS viruses has been limited. LCMV infection induces cerebral expression of IP-10, RANTES, and MCP-1 at 3 days post-infection with dramatic increase by 6 days, corresponding with the immunopathogenesis of LCMV infection (Asensio and Campbell, 1997). Either live or UV-inactivated Newcastle Disease Virus (NDV) induces RANTES and IP-10 expression in primary cultures of rat astrocytes and microglia (Fisher *et al*, 1995). Coordinated regulation of chemokine expression has been more extensively studied in chronic, relapsing experimental autoimmune encephalomyelitis (Ch-R EAE). Following active immunization, levels of MCP-1, MIP-1α, IP-10, GRO-α, and RANTES, were elevated in initial attacks of EAE and during the first relapse of disease, but returned to baseline or near baseline during remission of CNS inflammation (Glabinski *et al* 1997b). Using adoptive transfer, Karpus and Kennedy (1997) demonstrated persistent elevation of MIP-1α and RANTES

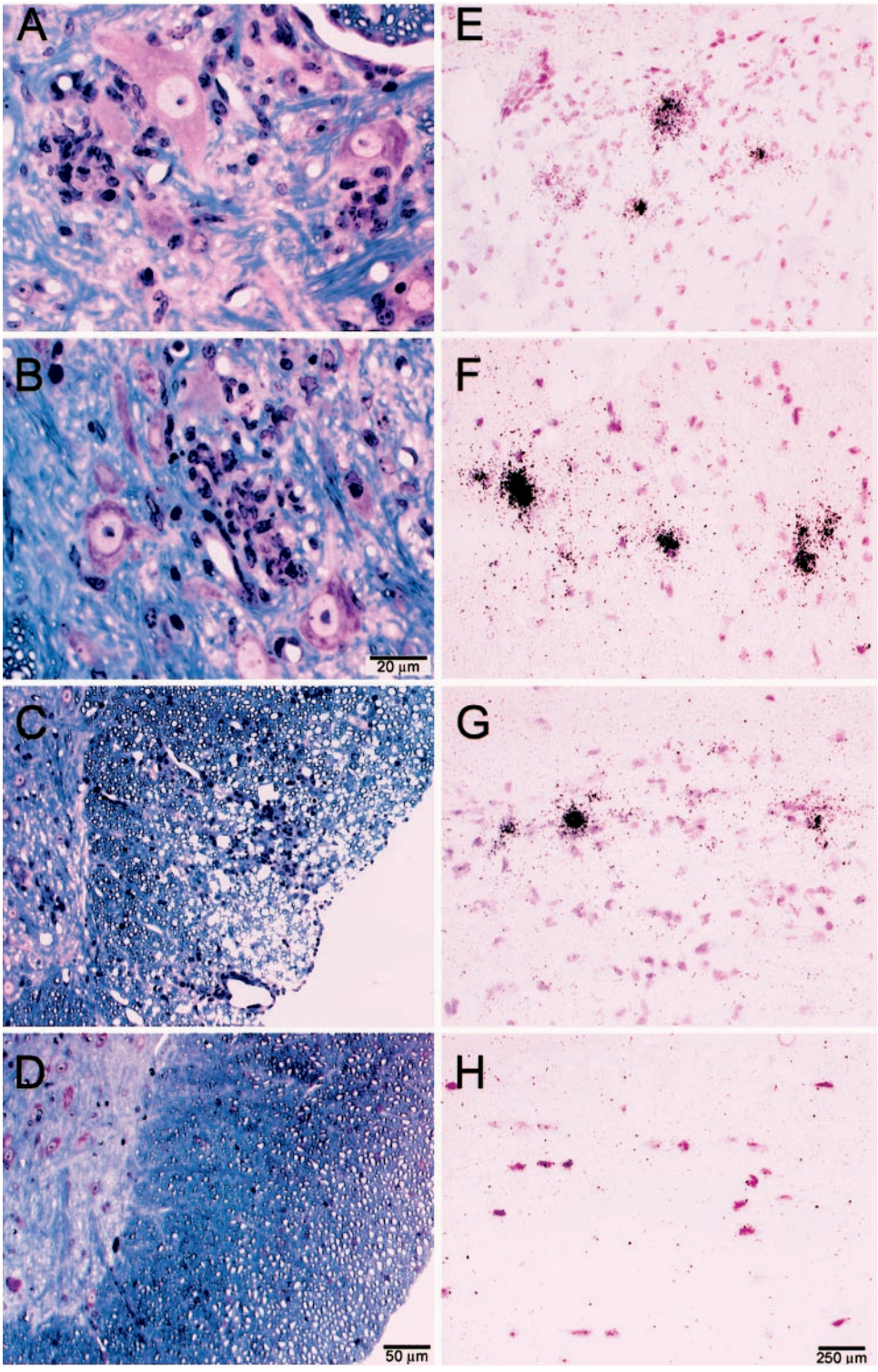

Figure 4 TMEV-infection results in acute inflammation in the gray matter of all strains, and chronic demyelinating disease and viral persistence in susceptible strains. Glycol methacrylate-embedded spinal cord sections obtained from B10.M (**A,C**) and B10 (**B,D**) mice infected for 5 (**A,B**) and 45 (**C,D**) days were stained with cresyl violet and modified erichrome stain. At 5 days post-infection, lymphocytic inflammation and neurophagia were detected in the gray matter of both B10.M (**A**) and B10 (**B**) mice. By 45 days following infection focal demyelinating lesions with perivascular and parenchymal infiltration were observed in B10.M mice (**C**), but not B10 mice (**D**). *In situ* hybridization with a ^{35}S-labeled probe specific for the VP1 region of TMEV demonstrates TMEV mRNA in the spinal cord gray matter of B10.M (**E**) and B10 (**F**) mice 5 days following infection. At 45 days, during the chronic demyelinating phase, virus mRNA was detected in the white matter of B10.M mice (**G**), but had been completely cleared from the spinal cords of B10 mice (**H**).

during initial attacks of EAE and the first remission, whereas only MCP-1 was detected during the relapse. The resurgence in chemokine expression and clinical relapses in Ch-R EAE were associated with epitope spreading to new myelin antigens (Yu *et al*, 1996). A similar resurgence in the TMEV-infected mice is probably due to the transition of viral replication from the gray to the white matter of the spinal cord.

The potential of chemokines as targets for therapeutic interventions has been demonstrated by studies of disease in both the CNS and peripheral organs. Infection with coxsackie virus B3 (CVB3) induced moderate to severe myocarditis, characterized by mononuclear cell infiltrate and cytolysis, in wild type mice but not mice with targeted disruption of the gene for MIP-1α (Cook *et al*, 1995). MIP-1α-deficient mice also developed reduced pulmonary inflammation and edema following influenza virus infection (Cook *et al*, 1995). In one study antibodies to MIP-1α, but not MCP-1, prevented and treated initial attacks after passive transfer of EAE (Karpus *et al*, 1995). In a subsequent study, treatment with anti-MCP-1 reduced the severity of relapses (Karpus and Kennedy, 1997). Therefore, chemokine-based therapies are potentially promising avenues for future research.

Materials and methods

Virus
The Daniel's strain of TMEV was used for all experiments. The passage history has been described previously (Lehrich *et al* 1976).

Mice
Mice susceptible (B10.M-*H2*^{f}/Sn) and resistant (C57BL/10J) to TMEV-induced demyelinating disease were obtained from Jackson Laboratories (Bar Harbor, ME). Mice 6–8 weeks old were injected intracerebrally with 2×10^6 p.f.u. of virus in 10 μl. Mice were sacrificed by injection of 10-mg pentobarbital (i.p.) 5, 21, and 45 days post-infection which corresponded with severe CNS inflammation and peak virus replication (day 5), virus clearance in resistant strains (day 21), and a demyelinating phase in susceptible strains (day 45) (Rodriguez and David, 1985). Handling of all animals conformed to both the National Institutes of Health and Mayo institutional guidelines.

RNA extraction
Brains (divided into three coronal sections) and spinal cords were frozen in liquid nitrogen chilled isopentane and stored in liquid nitrogen. Two 30 m stat sections of each tissue per animal were stored in sterile 1.5 ml tubes at -80°C. 250 μl of TRIzol™ (Gibco-BRL) were added to spinal cord sections and 1 ml to brain sections. Tissue sections were then homogenized and chloroform extraction was performed according to manufacturer's instructions. RNA was precipitated with isopropanol, using 20 mg/ml glycogen (Boehringer-Mannheim) as a carrier at -20°C overnight. RNA pellets were washed with 80% ethanol, air dried, then resuspended in sterile MilliQ H_2O. RNA concentration was determined by spectrophotometry and 1 μg of RNA was DNase treated (Gibco-BRL) according to manufacturer's instruction.

Reverse transcription coupled PCR
First strand cDNA was synthesized using 1 ug of DNase treated RNA, oligo dT primers, and Super-Script II™ (Gibco-BRL) according to manufacturer's instructions. The product of this reaction was amplified by PCR using primer pairs and Taq DNA polymerase (Boehringer Mannheim Corp.) Primer pair sequences are as follows; MCP-1 forward, 5′-ATCCCAATGAGTAGGCTGGAGAGC-3′, MCP-1 backward 5′-AAGGCATCACAGTCCGAGTCACAC-3′, RANTES forward, 5′-TTTGCCTACCTCTCCCTA-GAGCTG-3′, RANTES backward, 5′-ATGCC-GATTTTCCCAGGACC-3′ GRO-α forward 5′-TCGCTTCTCTGTGCAGCGCT-3′, GRO-α backward 5′-GTGGTTGACACTTAGTGGTCTC-3′, PCR conditions were set as follows: first denaturation, 94°C, 3 min; annealing, 60°C for 1 min; extension, 72°C, 1 min; denaturation 94°C 1 min. Optimal [Mg^{2+}] was empirically determined to be 1.5 mM for all three primer pairs. Mid-exponential point of the PCR cycle curve was 24 cycles for MCP-1, 25 cycles for RANTES and GRO-α.

Dot-blot hybridization analysis of chemokine cDNA
PCR reaction products were denatured in 2 M NaOH, 1 M Tris/HCL pH 7.6 at 80°C, 15 min, and quenched on ice for 1 min. Samples were diluted in $6 \times$ SSC, and transferred to a nylon membrane using a vacuum dot-blot manifold. Membranes were UV cross-linked and subjected to DNA hybridization analysis as follows; prehybridization with cDNA probes were generated from gel-purified cDNA inserts (Glabinski *et al*, 1997b) and labeled with [^{32}P] by random-priming (High Prime, Boehringer Mannheim). Hybridization signal was quantitated using a PhosphorImager (Molecular Dynamics) and expressed as arbitrary units. Statistical significance is reported at $P < 0.05$ using the Student's *t*-test. Messenger RNA levels, as determined by these assays, correspond closely to concentrations of chemokine protein (Glabinski *et al*, 1997b). These assays have been extensively validated in multiple models of CNS and PNS pathology (Glabinski *et al*, 1995, 1996, 1997a, 1998, 1999; Chien *et al* (unpublished observations); Ransohoff *et al*, 1993, 1997; Robinson *et al*, 1998).

Morphological analysis of CNS tissues
Mice were perfused by intracardiac puncture with Trump's fixative (phosphate buffered 4% formalde-

hyde with 1.0% glutaraldehyde, pH 7.2) (Rodriguez and David, 1985). Brains were cut into three coronal sections, embedded in paraffin, stained with hematoxylin and eosin, and the cerebellum, brain stem, hippocampus, striatum, cerebral cortex, corpus callosum, and meninges were graded independently for the presence of inflammation, demyelination and necrosis on a four-point scale. Scores were assessed as follows: 0=no pathology; 1=minimal inflammation with perivascular infiltration; 2=moderate inflammation with parenchymal infiltration but no loss of tissue architecture; 3=intense inflammation with definite parenchymal injury (loss of tissue architecture, demyelination, cell death, neurophagia, neuronal vacuolation); and 4=intense inflammation with obvious necrosis (complete loss of all tissue elements with associated cellular debris). Meningeal inflammation was assessed and graded as follows: 0=no inflammation; 1=one cell layer of inflammation, 2=two cell layers of inflammation; 3=three cell layers of inflammation; 4=four or more cell layers of inflammation. The area with maximal extent of tissue damage was used for assessment of each brain region. Spinal cords were sectioned into 1 mm transverse blocks, and every third block was embedded in paraffin for immunostaining or osmicated and embedded in JB-4 (Polysciences Inc., Warrington, PA.) (Rodriguez and David, 1985) for analysis of demyelination. Each quadrant from 12–15 spinal cord transverse sections per mouse was analyzed for the presence or absence of demyelination and inflammation. Data are expressed as the per cent of quadrants containing the pathologic finding.

In situ *hybridization*

In situ hybridization for TMEV RNA was conducted as described previously (Njenga *et al*, 1996). Slides were hybridized with ^{35}S-labeled 363-bp (nucleotides 3306–3668) cDNA probes corresponding to VP1 of TMEV (DA strain) (Ohara *et al*, 1988). The cDNA probes were obtained by double digesting the VP1 plasmid with *kpn*I and *Sal*I restriction enzymes and radiolabeling the probes with between 0.5×10^8 and 0.8×10^8 c.p.m. of [^{35}S]dATP/μg of DNA by nick translation.

Abbreviations

Bst, brainstem; Cco, corpus callosum; Crb, cerebellum; Cor, cerebral cortex; Hip, hippocampus; IP-10, interferon-γ-inducible protein of 10 kd, MCP-1, monocyte chemoattractant protein-1; Men, meninges; RANTES, regulated on activation, normal T-cell expressed and secreted cytokine; Stm, Striatum; TMEV, Theiler's murine encephalomyelitis virus.

Acknowledgements

This work was supported by the National Institutes of Health grants: RO1 NS24180, and RO1 NS32129 (to M Rodriguez) and RO1 NS32151 (RM Ransohoff) and the National Multiple Sclerosis Society grant RG 2203 B-6 (M Rodriguez) and RG 2362 B-5 (RM Ransohoff), and the generous contributions of Ms K Peterson and the Williams Family Fund for Multiple Sclerosis Research.

References

Asensio VC, Campbell IL (1997). Chemokine gene expression in the brains of mice with lymphocytic choriomeningitis. *J Virol* **71:** 7832–7840.

Carr MW, Roth SJ, Luther E, Rose SS, Springer TA (1994). Monocyte chemoattractant protein 1 acts as a T-lymphocyte chemoattractant. *Proc Natl Acad Sci USA* **91:** 3652–3656.

Cook DN, Beck MA, Coffman TM, Kirby SL, Sheridan JF, Pragnell IB, Smithies O (1995). Requirement of MIP-1 alpha for an inflammatory response to viral infection. *Science* **269:** 1583–1585.

Drescher KM, Pease LR, Rodriguez M (1997). Antiviral immune responses modulate the nature of central nervous system (CNS) disease in a murine model of multiple sclerosis. *Immunol Rev* **159:** 177–193.

Fisher SN, Vanguri P, Shin HS, Shin ML (1995). Regulatory mechanisms of MuRantes and CRG-2 chemokine gene induction in central nervous system glial cells by virus. *Brain, Behav Immunity* **9:** 331–344.

Glabinski A, Krakowski M, Owens T, Ransohoff RM (1999). Chemokine expression in GKO mice (lacking interferon-gamma) with experimental autoimmune encephalomyelitis. *J Neurovirol* **5:** 95–102.

Glabinski A, Tuohy V, Ransohoff RM (1998). Expression of chemokines RANTES, MIP-1α and GRO-α correlates with inflammation in acute experimental autoimmune encephalomyelitis. *Neuroimmunomodulation* **5:** 166–171.

Glabinski AR, Balasingam V, Tani M, Kunkel SL, Strieter RM, Yong VW, Ransohoff RM (1996). Chemokine monocyte chemoattractant protein-1 is expressed by astrocytes after mechanical injury to the brain. *J Immunol* **156:** 4363–4368.

Glabinski AR, Tani M, Strieter RM, Tuohy VK, Ransohoff RM (1997a). Synchronous synthesis of alpha- and beta-chemokines by cells of diverse lineage in the central nervous system of mice with relapses of chronic experimental autoimmune encephalomyelitis. *Am J Pathol* **150:** 617–630.

Glabinski AR, Tani M, Strieter RM, Tuohy VK, Ransohoff RM (1997b). Synchronous synthesis of alpha- and beta-chemokines by cells of diverse lineage in the central nervous system of mice with relapses of chronic experimental autoimmune encephalomyelitis. *Am J Pathol* **150:** 617–630.

Glabinski AR, Tan M, Tuohy VK, Tuthill RJ, Ransohoff RM (1995). Central nervous system chemokine mRNA accumulation follows initial leukocyte entry at the onset of acute murine experimental autoimmune encephalomyelitis. *Brain, Behav Immunity* **9:** 315–330.

Karpus WJ, Kennedy KJ (1997). MIP-1alpha and MCP-1 differentially regulate acute and relapsing autoimmune encephalomyelitis as well as Th1/Th2 lymphocyte differentiation. *J Leuk Biol* **62:** 681–687.

Karpus WJ, Lukacs NW, McRae BL, Strieter RM, Kunkel SL, Miller SD (1995). An important role for the chemokine macrophage inflammatory protein-1 alpha in the pathogenesis of the T cell-mediated autoimmune disease, experimental autoimmune encephalomyelitis. *J Immunol* **155:** 5003–5010.

Lehrich JR, Arnason BG, Hochberg FH (1976). Demyelinative myelopathy in mice induced by the DA virus. *J Neurol Sci* **29:** 149–160.

Lira SA, Zalamea P, Heinrich JN, Fuentes ME, Carrasco D, Lewin AC, Barton DS, Durham S, Bravo R (1994). Expression of the chemokine N51/KC in the thymus and epidermis of transgenic mice results in marked infiltration of a single class of inflammatory cells. *J Exp Med* **180:** 2039–2048.

Monteyne P, Bureau JF, Brahic M (1997). The infection of mouse by Theiler's virus: from genetics to immunology. *Immunol Rev* **159:** 163–176.

Njenga MK, Asakura K, Hunter SF, Wettstein P, Pease LR, Rodriguez M (1997). The immune system preferentially clears Theiler's virus from the gray matter of the central nervous system. *J Virol* **71:** 8592–8601.

Njenga MK, Pavelko KD, Baisch J, Lin X, David C, Leibowitz J, Rodriguez M (1996). Theiler's virus persistence and demyelination in major histocompatibility complex class II-deficient mice. *J Virol* **70:** 1729–1737.

Ohara Y, Stein S, Fu J, Stillman L, Klaman L, Roos RP (1988). Molecular cloning and sequence determination of DA strain of Theiler's murine encephalomyelitis virus. *Virology* **164:** 245–255.

Ransohoff RM, Glabinski A, Tani M (1996). Chemokines in immune-mediated inflammation of the central nervous system. *Cytokine Growth Factor Rev* **7:** 35–46.

Ransohoff RM, Hamilton TA, Tani M, Stoler MH, Shick HE, Major JA, Estes ML, Thomas DM, Tuohy VK (1993). Astrocyte expression of mRNA encoding cytokines IP-10 and JE/MCP-1 in experimental autoimmune encephalomyelitis. *FASEB J* **7:** 592–600.

Ransohoff RM, Tani M, Glabinski A, Chernosky K, Krivacio K, Peterson J, Chien HF, Trapp B (1997). Chemokines and chemokine receptors in model neurological pathologies: molecular and immunocytochemical aproaches. *Methods Enzymol* **287:** 319–348.

Robinson SM, Tani M, Strieter RM, Ransohoff RM, Miller RH (1998). The chemokine GRO-α amplifies PDGF-induced proliferation of spinal cord oligodendrocyte progenitors. *J Neurosci* **18:** 10457–10463.

Rodriguez M, David CS (1985). Demyelination induced by Theiler's virus: influence of the H-2 haplotype. *J Immunol* **135:** 2145–2148.

Rodriguez M, David CS, Pease LR (1987). The contribution of MHC gene products to demyelination by Theiler's virus. In: *H-2 antigens*. David CS (ed). Plenum Publishing Corp, New York, pp 747–756.

Rollins BJ, Walz A, Baggiolini M (1991). Recombinant human MCP-1/JE induces chemotaxis, calcium flux, and the respiratory burst in human monocytes. *Blood* **78:** 1112–1116.

Schall TJ, Bacon K, Toy KJ, Goeddel DV (1990). Selective attraction of monocytes and T lymphocytes of the memory phenotype by cytokine RANTES. *Nature* **347:** 669–671.

Tani M, Ransohoff RM (1994). Do chemokines mediate inflammatory cell invasion of the central nervous system parenchyma? *Brain Pathol* **4:** 135–143.

Taub DD, Lloyd AR, Conlon K, Wang JM, Ortaldo JR, Harada A, Matsushima K, Kelvin DJ, Oppenheim JJ (1993). Recombinant human interferon-inducible protein 10 is a chemoattractant for human monocytes and T lymphocytes and promotes T cell adhesion to endothelial cells. *J Exp Med* **177:** 1809–1814.

Tsunoda I, Fujinami RS (1996). Two models for multiple sclerosis: experimental allergic encephalomyelitis and Theiler's murine encephalomyelitis virus. *J Neuropathol Exp Neurol* **55:** 673–686.

Yoshimura T, Robinson EA, Tanaka S, Appella E, Kuratsu J, Leonard EJ (1989). Purification and amino acid analysis of two human glioma-derived monocyte chemoattractants. *J Exp Med* **169:** 1449–1459.

Yu M, Johnson JM, Tuohy VK (1996). A predictable sequential determinant spreading cascade invariably accompanies progression of experimental autoimmune encephalomyelitis: a basis for peptide-specific therapy after onset of clinical disease. *J Exp Med* **183:** 1777–1788.